CORRELATED FAST TIME STRUCTURES AT MILLIMETER WAVES AND HARD X-RAYS DURING A SOLAR BURST

P. KAUFMANN[1], G. TROTTET[2], C. G. GIMÉNEZ DE CASTRO[1], J. E. R. COSTA[1], J.-P. RAULIN[1], R. A. SCHWARTZ[3] and A. MAGUN[4]

[1]*CRAAE, Instituto Presbiteriano Mackenzie, Rua da Consolação 896, 01302-907, S. Paulo, SP, Brazil;*

[2]*Observatoire de Paris, Section de Meudon, DASOP, CNRS-UMR 8645, F-92195 Meudon, France*

[3]*Raytheon ITSS and Laboratory for Astronomy and Solar Physics, NASA/Goddard Space Flight Center, Code 682, Greenbelt, MD 20771, U.S.A.*

[4]*Institute of Applied Physics, University of Bern, Sidlestr. 5, CH-3012, Switzerland*

(Received 8 February 2000; accepted 15 July 2000)

Abstract. We present an analysis of the time profiles detected during a solar impulsive flare, observed at one-millimeter radio frequency (48 GHz) and in three hard X-ray energy bands (25–62, 62–111, and 111–325 keV) with high sensitivity and time resolution. The time profiles of all emissions exhibit fast time structures of 200−300 ms half power duration which appear in excess of a slower component varying on a typical time scale of 10 s. The amplitudes of both the slow and fast variations observed at 48 GHz are not proportional to those measured in the three hard X-ray energy bands. However, the fast time structures detected in both domains are well correlated and occur simultaneously within 64 ms, the time resolution of the hard X-ray data. In the context of a time-of-flight flare model, our results put strong constraints on the acceleration time scales of electrons to MeV energies.

1. Introduction

One of the critical issues for understanding electron acceleration during solar flares is to determine how quickly these particles are accelerated (Miller *et al.*, 1997). The most direct diagnostics of non-thermal electrons is the hard X-ray (HXR) and gamma-ray (GR) continuum emission which is believed to be the result of bremsstrahlung from sub-relativistic to relativistic electrons. For sub-relativistic electrons an upper limit on the acceleration time to $\sim$ 100 keV has been obtained from the analysis of the time evolution of the HXR emission observed during impulsive flares. Indeed, in the 25–100 keV energy range, the time profiles of most impulsive HXR bursts exhibit numerous pulses lasting a few hundreds of milliseconds (e.g., Kiplinger *et al.*, 1983; Hurley *et al.*, 1983; Desai *et al.*, 1987; Vilmer *et al.*, 1994, 1996; Machado *et al.*, 1993; Aschwanden, Schwartz, and Alt, 1995). This supports the early suggestion by Kaufmann *et al.* (1980, 1985) that the flare production of non-thermal electrons may result from the superposition of discrete and fast acceleration events which occur at various repetition rates (e.g., Vilmer and Trottet, 1997, and references therein). Moreover, such short time scales

Solar Physics **197:** 361–374, 2000.

imply that the HXR emission is produced through thick-target interaction so that the rise time of an HXR pulse, typically 100–1000 ms (Vilmer *et al.*, 1996), can be considered as an upper limit of the electron acceleration time to an energy of $\sim$ 100 keV (Miller *et al.*, 1997).

The acceleration time of electrons to relativistic energies can be in principle estimated in the same way by using the time profile of the flare associated GR continuum emission. At energies ranging from a few MeV to a few tens of MeV, there are rare examples of GR peaks, unresolved with time resolutions of 0.5 s (Pelaez *et al.*, 1992), 1 s (Talon *et al.*, 1993; Kurt, Akimov, and Leikov, 1996) and 2 s (Forrest and Chupp, 1983). This suggests that the acceleration time to MeV energies is no more than a few seconds. However, the sensitivity of GR detectors was insufficient to investigate shorter time scales. A more sensitive diagnostic is the centimeter–millimeter (cm–mm) radio emission which is the result of gyrosynchrotron radiation from electrons with energies above a few hundred keV (e.g., White *et al.*, 1992; Kundu *et al.*, 1994; Ramaty *et al.*, 1994; Trottet *et al.*, 1998; Raulin *et al.*, 1999). There are numerous examples showing the existence of sub-second pulses in the time profiles of cm–mm bursts (e.g., Kaufmann *et al.*, 1980; Raulin *et al.*, 1998). However, for frequencies where emission arises from an optically thin source, the observed intensity depends, in a simple way, on both the magnetic field strength and the instantaneous number of radiating electrons. Thus the correlation between pulses observed in the HXR and cm–mm domains should, in principle, allow us to eliminate flux variations induced by changes of the magnetic field strength alone. At present only a few flares have been analyzed with high time resolution in both wavelength domains. One event observed by the SMM/HXRBS experiment at photon energies $>$ 25 keV has shown sub-second time structures coincident with fast structures at cm–mm-waves. However, the time resolution of the X-ray data was limited to 128 ms (Kaufmann *et al.*, 1985). Another event detected in the same photon energy range by *Hinotori*/HXT has shown sub-second time structures with suggestive correspondences in the cm–mm radio emission (Takakura *et al.*, 1983; Zodi Vaz *et al.*, 1985). However, the HXR measurements were restricted to photon energies dominated by the 25 keV emission where the thermal contribution might still be significant, blurring the finer time structures.

In this paper we present an analysis of the 8 February 1993 impulsive solar burst at 17:08 UT which compares HXR measurements in the 25–62 keV, 62–111 keV, and 111–325 keV energy bands, made with high sensitivity and time resolution (64 ms) by the CGRO/BATSE experiment, to the 48 GHz emission detected by the 13.7-m Itapetinga radio-telescope with a sensitivity of 0.04 s.f.u. (r.m.s.) and a time resolution of 1 ms. The time resolution of these data is high enough to allow us to clearly identify sub-second 48 GHz time structures which are correlated to HXR pulses detected at photon energies where the contribution of the thermal X-ray emission is negligible. The relevance of the time characteristics of these pulses with respect to the electron acceleration timescale to relativistic energies is

discussed in the context of the time-of-flight (TOF) flare model (Brown, Conway, and Aschwanden, 1998, and references therein).

2. Instrumentation

The 48 GHz observations of the 8 February 1993 solar burst at $\sim$ 17:08 UT were obtained by the Itapetinga 13.7-m radio telescope with a time resolution of 1 ms and a sensitivity of 0.04 s.f.u. (Kaufmann *et al.*, 1982). The multiple receiver focal array produces five beams, with half power width of 2 arc minutes which partially overlap (Georges *et al.*, 1989; Herrmann *et al.*, 1992; Costa *et al.*, 1995). When a significant signal is detected in at least three of the beams, the position of the 48 GHz emitting source can, in principle, be determined (Giménez de Castro *et al.*, 1999, and references therein). The 8 February 1993 burst emission was, however, significantly detected in only one of the beams. The 48 GHz data are therefore treated as being obtained by a single beam closely pointed to the burst source.

The HXR observations were obtained by the CGRO/BATSE experiment which is described in detail in Pendleton *et al.* (1995). In the present study we have used the DISCSC (Discriminator Science Data) burst trigger data which are recorded in four energy channels (25–62, 62–111, 111–325 keV, and $>$ 325 keV) with a uniform time resolution of 64 ms.

3. Data Analysis

The 8 February 1993 event at 17:08 UT was associated with a 1B optical flare (GOES C7.1) which occurred in NOAA region 7420 located at S03/E26 (*Solar-Geophysical Data* reports). A weak microwave burst was also reported with maximum flux densities of 58 s.f.u. (1 s.f.u.$=10^{-22}$ W m^{-2} Hz^{-1}) and 180 s.f.u. at 2.695 GHz and 8.8 GHz, respectively. The maximum flux density measured at 48 GHz by the Itapetinga instrument was approximately 20 s.f.u. This indicates that the turnover frequency of the cm–mm radio spectrum is below 48 GHz. In the following we thus consider that the 48 GHz emission belongs to the optically thin part of the cm–mm radio spectrum.

The 48 GHz radio burst starts at $\sim$ 17:07:50 UT. This onset time corresponds to the first BATSE burst trigger data indicating that the onset of the HXR emission was close to that of the 48 GHz radio emission. However, the records stored by BATSE during the first two seconds are not reliable. The HXR event consists of an initial strong impulsive burst lasting until $\sim$ 17:08:35 UT with significant emission up to 325 keV. This impulsive burst is followed by a weaker increase of the HXR emission lasting until $\sim$ 17:12:18 UT which is not detected above 111 keV at a time resolution of 64 ms. This latter HXR emission will not be considered in this study. The time profiles of the background-subtracted HXR rates and of the 48 GHz flux

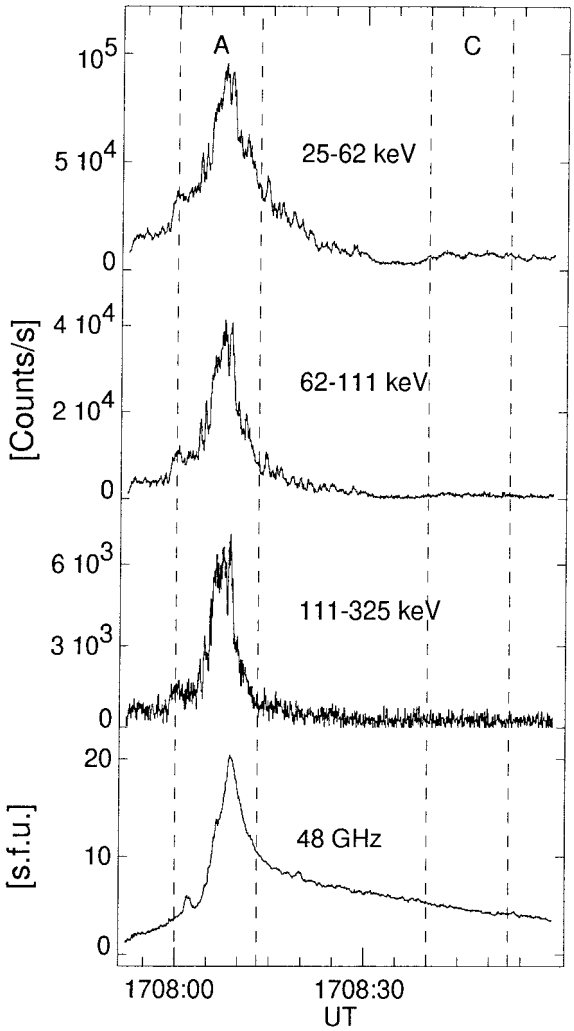

Figure 1. Time profiles of the background-subtracted count rates measured by BATSE in three energy channels and of the 48 GHz radio flux density observed by the Itapetinga radiotelescope. All data are shown with a time resolution of 64 ms. The time intervals marked A and C correspond to the time intervals used to study the fast time variations and to control the results (see text).

density are shown on Figure 1 with a time resolution of 64 ms from 17:07:52 UT until 17:09 UT. The time profile of the 48 GHz flux density is globally similar to the time evolution of the HXR count rates measured in the three energy channels: both emissions rise together and show a rapid decay until $\sim$ 17:08:13 UT followed by a slower one. However, the ratio of the HXR count rate to the 48 GHz flux density varies during the event.

Figure 1 further shows that the HXR time histories as well as the time profile of the 48 GHz emission exhibit both slow variations on a $\sim$ 10 s time scale

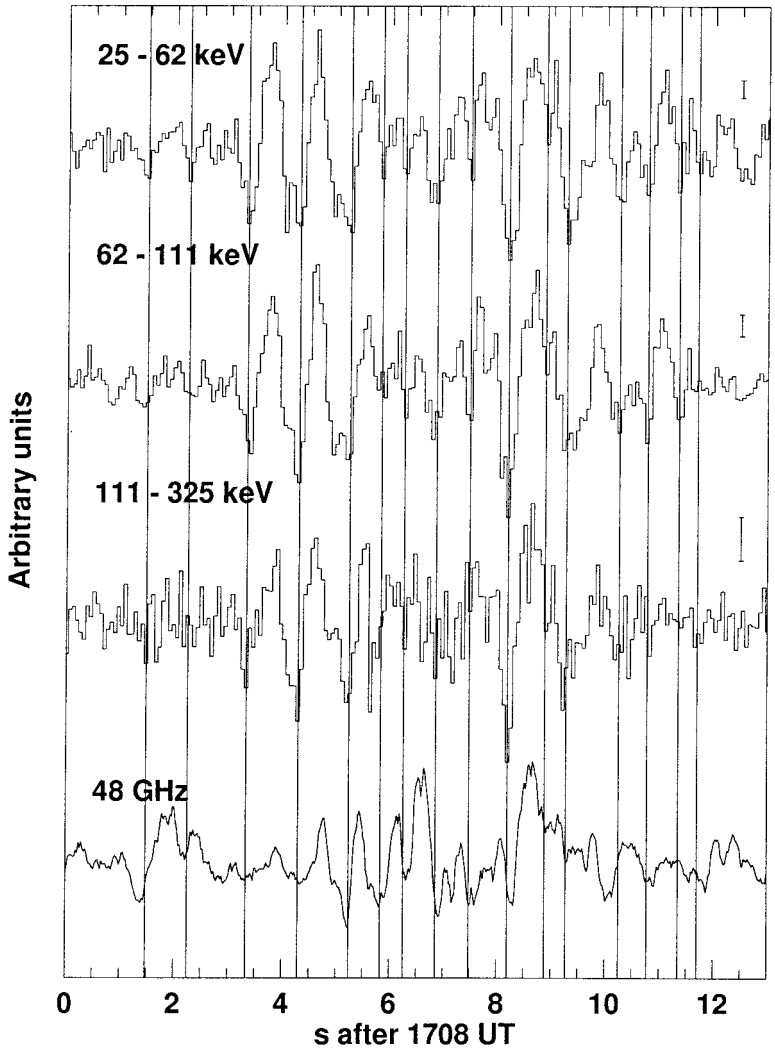

Figure 2. Time profiles of the HXR and 48 GHz fast components obtained with a time resolution of 64 ms. The vertical lines correspond to the minima of the 25–62 keV HXR fast variations.

(bulk emission) and fast pulses ($\sim$ 1 s). In order to remove the slow variation a one-second running mean has been subtracted from the three HXR rates and the 48 GHz emission, integrated to 64 ms (Costa *et al.*, 1990). Figure 2 shows the remaining HXR and 48 GHz pulses during the interval of time marked A on Figure 1 (17:08 UT to 17:08:13 UT). This time interval has been chosen because there are no HXR pulses before its beginning and because its end corresponds to the end of the impulsive burst in the 111–325 keV HXR channel. Furthermore we did not consider the slow decay (17:08:13–17:08:35 UT) where thermal emission may substantially contribute to the 25–62 keV HXR and 48 GHz emissions. On

the basis of Figure 2 and of a detailed examination of the fast and slow HXR and 48 GHz time variations, the following statements can be made:

– There is a clear correspondence between some significant HXR pulses detected in one or more energy channels and 48 GHz pulses. However, there are also 48 GHz pulses which have no or only marginal correspondence in the HXR domain, in particular at the beginning of interval A.

– The vertical lines drawn in Figure 2 mark the start times of individual pulses or groups of pulses taken as the minima of the HXR emission in the lowest energy channel. It clearly appears that, within the 64 ms time resolution, correlated pulses have similar times in the different HXR channels and at 48 GHz.

– The contrast between the HXR pulses and the smooth HXR rates has a tendency to increase with increasing photon energy. It is $\sim$15–35%, $\sim$20–60%, and $\sim$20–80% in the 25–62 keV, 62–111 keV, and 111–325 keV, respectively. At 48 GHz, the contrast between pulses and smooth variations ($\sim$ 5–15%) is somewhat lower.

– For both the bulk emission and the pulses the ratios of the HXR rates to the 48 GHz flux density vary with time.

– The characteristic e-folding rise and fall times of the pulses, 150–200 ms, are similar at both HXR and mm-wavelengths and their half-power durations lay in the range 200–300 ms. This is in agreement with the results of previous studies (e.g., Vilmer *et al.*, 1996, and references therein).

We therefore conclude that, within the time resolution of 64 ms, the HXR and 64 GHz time profiles exhibit sub-second time structures which are simultaneous. This is further demonstrated by Figure 3 which shows the coefficients of cross-correlation between the HXR and 48 GHz emissions, for the three energy channels. These coefficients are maximum at a value of about 0.4 for a time lag of 0 to 64 ms. We consider that such a correlation is significant. Indeed: (i) the low values of the coefficients of correlation mostly reflect that the amplitudes of the HXR and 48 GHz pulses are not proportional and that some of the HXR pulses are not or marginally significant; (ii) for the interval of time marked C in Figure 1, where no fast variations are observed, the coefficients of correlation are close to zero. Finally, Figure 4 shows that the most intense HXR single structures correspond to single 48 GHz structures detected with the original 1 ms time resolution. This indicates that, within the time resolution of 64 ms, some of the HXR pulses are resolved.

The fact that the ratio, R, between the HXR and mm-waves emissions varies through the event for both the fast and slow variations is a natural consequence of the fact that both emissions are radiated by electrons of different energies through different processes. Indeed it has been shown that the electron spectrum hardens above a break energy in the $\sim$ 300 keV–1 MeV range (Vestrand, 1988; Trottet *et al.*, 1998; Vilmer *et al.*, 1999). A change of this energy break in the course of the burst, as was already observed (Trottet *et al.*, 1998), will induce a change of R. Variations of R may also result from changes of the magnetic field strength because the location of the 48 GHz source may not remain the same during the event (e.g.,

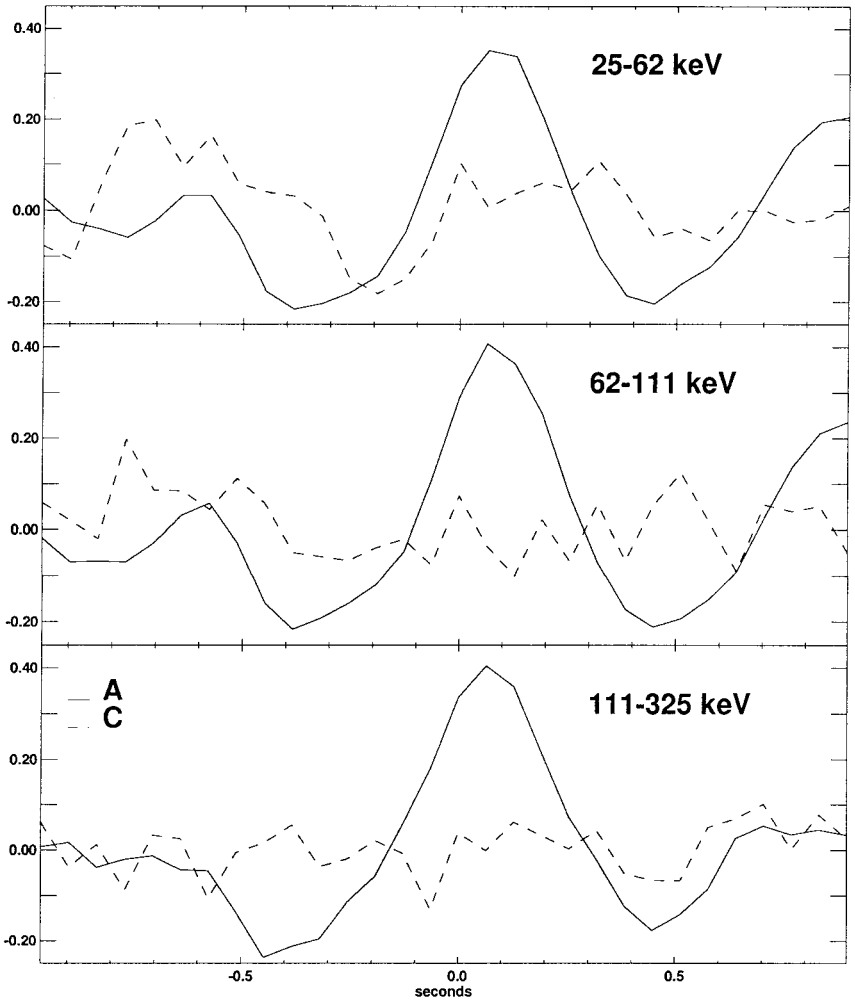

Figure 3. Cross-correlation coefficient versus the time lag between the HXR and 48 GHz fast variations shown in Figure 2 for the three BATSE energy channels. For comparison the dashed lines show the cross-correlation coefficients obtained for the time interval marked C in Figure 1.

Correia *et al.*, 1995; Raulin *et al.*, 1998, 2000). Unfortunately, dynamic spectra of the microwave pulses are not available so that changes in the ratio R due to an increase in self absorption of the mm-emission at pulse maximum can not be excluded.

4. Discussion

We have shown that the time profiles of the 25–325 keV HXR emission detected in three energy channels by CGRO/BATSE, during the 8 February 1993 solar burst at

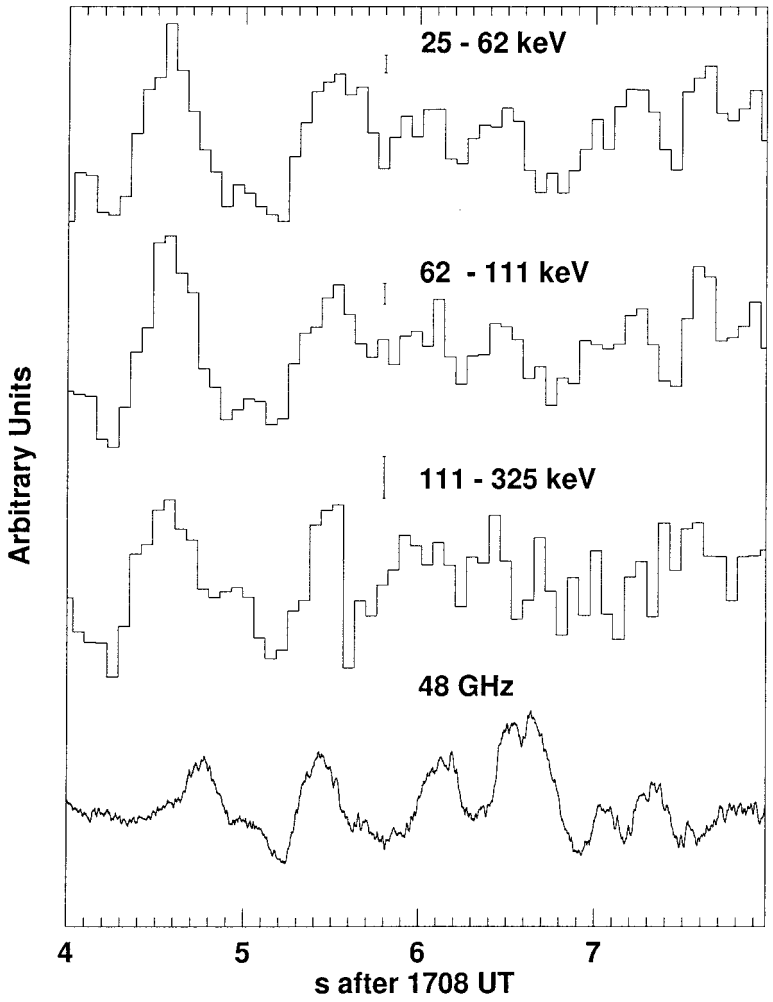

Figure 4. Expanded view of Figure 2 from 4 to 8 s after 17:08:00 UT. The time resolution of the 48 GHz data is 1 ms.

$\sim$ 17:08 UT, are globally similar to the time profile of the 48 GHz radio emission observed by the Itapetinga radiotelescope. In addition to slow variations on time scales of $\sim$ 10 s, pulses of sub-second duration (typically 200–300 ms at half power) were found to occur simultaneously within 64 ms in both wavelength domains. In the absence of cm–mm-λ spectral observations and of HXR and/or radio imaging observations, the present data set does not provide sufficient constraints to perform a fully quantitative interpretation of our findings. In the following we thus qualitatively discuss our results in the framework of models where the millimeter radio source is the result of: (1) gyrosynchrotron emission in the coronal part of the flare loops and (2) inverse Compton losses in a compact synchrotron source.

HXR imaging observations around a few tens of keV have revealed that the bulk of the impulsive HXR emission is produced at conjugate footpoints of flaring loops with typical sizes of a few 10^9 cm (e.g., Duijveman, Hoyng, and Machado, 1982; Sakao *et al.*, 1992). For an impulsive burst like the present event, it is likely to assume that the 30–150 keV HXR emission is the result of thick-target electron bremsstrahlung. Indeed, stereoscopic observations of impulsive HXR events indicate that more than 90% of the impulsive HXR emission is produced at altitudes ≤ 2500 km above the photosphere (Kane *et al.*, 1982), i.e., in the low corona or upper chromosphere. Thick-target interactions imply that the electron collisional energy loss time is much shorter than the fastest time scale ($\sim$ 200 ms) of the HXR emission. For 150 keV electrons this is realized for target densities larger than 10^{12} cm^{-3}. The thick-target HXR emission evolves in time like the electron flux F (electrons s^{-1} keV^{-1}) entering the target. If electrons are injected in the loop at a rate F_0 from a remote accelerator the time variations of F, thus of the HXR emission, reflects both F_0 and time variations which result from electron propagation from the injection region to the HXR emitting site. In the absence of HXR imaging observations we assume that the injection region is near the top of a flare loop as suggested by observations of HXR coronal sources at the apex of soft X-ray flare loops (Masuda *et al.*, 1994) and of the synchronisation (within 1 s) of HXR sources at the conjugate footpoints of compact loops (Sakao, 1994). The propagation of electrons from the loop top to the loop footpoints is then achieved through a direct path for electrons with small initial pitch angles and through a magnetic mirror trap with subsequent escape through the loss cone due to pitch angle scattering. Collisional trap + precipitation models, where scattering is due to Coulomb collisions have been considered by, e.g., MacKinnon *et al.* (1983) and Aschwanden (1998). Aschwanden, Schwartz, and Dennis (1998) have applied such a model to numerous BATSE events but their Table 1 does not include the present burst. They made the crucial assumption that the injection of electrons from the accelerator occurs by pulsed injections synchronised in energy and pitch angles. The main findings, relevant to the present study, are: (i) energy dependent delays in HXR peak times with respect to the electron injection peak time result from delays induced by the electron TOF through the loop which vary as $E^{-\frac{1}{2}}$ and delays related to the electron collisional trapping times which vary as $E^{\frac{3}{2}}$ where E is the electron energy; (ii) HXR pulses with shorter time scales than the trapping time will be smeared out so that the contrast between pulses and the smooth component decreases with energy. A further consequence of this model is that the decay time of the smooth component should increase with energy.

For the 8 February 1993 flare, (i) the *e*-folding decay time of the smooth HXR emission does not increase with energy instead it is somewhat longer for the 25–62 keV channel ($\sim$ 6 s) than for the 62–111 keV and 111–325 keV channels ($\sim$ 3 s) and (ii) the contrast between pulsed and smooth HXR emissions increases with increasing energy. This provides indications that collisional trapping does not play a major role during this event. This may be the case if for example: (1) the

convergence of the magnetic field is small; (2) all electrons are injected at small pitch angles; (3) the collisional trapping time of 150 keV electrons is shorter than $\sim$ 300 ms (half-power duration of HXR pulses) leading to a loop density larger than 6×10^{11} cm^{-3}; (4) pitch-angle diffusion is not due to collision but to other processes such as wave-resonant scattering (e.g., Trottet and Vilmer, 1984); and (5) the injection site is close to the interaction sites. The present data does not allow us to discriminate between these different possibilities. However, (3) and (5) describe situations close to direct injection from the accelerator into the thick-target source so that electron propagation is suppressed whereas points (1) and (4) depict cases where propagation effects are essentially due to the energy dependent TOF of electrons. Point (2) is unlikely unless the initial pitch angle of MeV electrons is not beamed along the magnetic field. Indeed electrons with small pitch angles will not radiate gyrosynchrotron radio emission (e.g., Klein and Trottet, 1984). Direct propagation of electrons from the injection site to the interaction site is only possible for electrons that have a collisional life time much larger than their loop transit time. For a loop half-length of 10^9 cm and initial mean pitch angle of 45 deg using Equation (1) in Aschwanden (1998) we find that 30 keV electrons implied a loop density lower than $\sim 2 \times 10^{11}$ cm^{-3}. For the chosen parameters the TOF difference for 30 keV and 150 keV electrons $\sim$ 68 ms is comparable to time resolution of the HXR data which is consistent with the absence of measurable energy dependent delays in the HXR peak times by just comparing the HXR time profiles (see Figures 1, 2, and 4).

In summary the BATSE 30–150 keV HXR observations of the 8 February 1993 flare are consistent with a pulsed injection of electrons synchronised in energy over a large range of pitch angles either from the top of loop with typical half-length of $\sim 10^9$ cm and density substantially lower than 2×10^{11} cm^{-3} or directly into the thick-target HXR emitting sources. For a pulsed injection synchronised in energy the data are not consistent with direct injection into the thick-target region because the smooth HXR component can only be explained if it is already present in the injection. On the contrary, direct propagation from the loop top to the loop footpoints of a nearly isotropic distribution of electrons will produce HXR pulses at the loop footpoints with longer duration than the injected electron pulses. This enlargement of the pulse duration decreases with increasing energy due to the decrease of the electron collision time with increasing energy (see, e.g., Emslie, 1983; Vilmer, Trottet, and Mackinnon, 1986). This provides a simple explanation for the existence of a smooth HXR emission when time between two peaks of electron injection is shorter than the enlargement of the pulse width due to propagation. Detailed calculation of such an effect is beyond the scope of this paper, however, for a pulse repetition rate of $\sim$ 1 s^{-1} the above condition is easily fulfilled for loop half length of $\sim 10^9$ cm and densities in the range of 10^{10}–10^{11} cm^{-3} (see Figure 1 in Emslie, 1983). This is furthermore consistent with the observed increase of the contrast of the pulsed to the smooth HXR components with energy. Such a pure TOF interpretation of the data puts strong constraints on the acceleration

mechanism. In particular it implies that the acceleration time to 150 keV must be far below 64 ms, the time resolution of the HXR data (Brown, Conway, and Aschwanden, 1998).

If the 48 GHz radio emission is the result of gyrosynchrotron radiation from relativistic electrons in the MeV region (e.g., Ramaty *et al.*, 1994), the millimeter source is most probably located in the coronal portion of the flare loop. For an optically thin source as the one observed here, the time profile of the radio emission mimics that of the instantaneous number of $\sim$ 1 MeV electrons $N_e(t)$ present in the radio emitting source. For direct precipitation $N_e(t)$ is given by the time integral of the injection rate of MeV electrons in the radio source over their TOF through this source which is shorter than $\sim$ 50 ms (TOF of 1 MeV electron through the 10^9 cm loop). Since the HXR and 48 GHz pulses are synchronized and show similar rise times and since the TOF of MeV electrons is substantially shorter than the pulse durations ($\sim$ 300 ms), the time profile of the 48 GHz emission varies nearly like the injection rate of MeV electrons in the radio source which mimics the injection rate of the 30–150 keV electrons in the thick target. As a consequence, the electron acceleration times to MeV energies must also be much shorter than 64 ms, the chosen time resolution to display the radio data. However, according to Brown, Conway and Aschwanden (1998) acceleration by a direct electric field or by a turbulent plasma wave field may be able to accelerate MeV electrons in microseconds. However, Brown, Conway, and Aschwanden (1998) have shown that 'there exists a range of time- and energy-dependent forms of electron acceleration spectrum variations (in which the injection spectrum softens with time for each HXR pulse) which can exactly mimic HXR data like those expected solely from time-of-flight differences'. Radio observations obtained at different microwave and millimeter wavelengths with a one millisecond time resolution, like those reported here, may provide a unique means to look for such variations of the electron acceleration spectrum.

As an alternative to the TOF interpretation it was proposed that fast time structures observed in the mm radio domain are due to compact synchrotron sources of high-energy electrons (Kaufmann *et al.*, 1985, 1986; McClements and Brown, 1986; Kaufmann, 1996). The energy of the relativistic electrons is reduced by inverse Compton effect on the synchrotron photon field, producing a fraction of the HXR fast time structures observed simultaneously with the mm-emission. The bulk of burst emission would therefore be due to gyrosynchrotron losses of mildly relativistic electrons resulting after the inverse Compton quenching which will also produce the HXR by bremsstrahlung at the denser regions of the solar atmosphere. The typical time scale of the fast pulses might then reflect the time required by the inverse Compton effect to reduce the electron energies (Kaufmann *et al.*, 1986). This possibility requires the formation of dense compact sources in order to get a significant efficiency of the inverse Compton effect. However, such an interpretation faces additional difficulties (see Vilmer, 1987). In particular, the population

of accelerated electrons must have a low-energy cut-off around 1 MeV and such a population may be difficult to produce.

5. Conclusions

In this study we have analyzed and compared the time evolutions of the HXR emission detected by CGRO/BATSE in the 25–325 keV energy range and of the mm-wave emission observed at 48 GHz by the Itapetinga radio-telescope during an impulsive solar flare. The time histories are globally similar in both wavelength domains and exhibit slow and fast variations on time scales of ~ 10 s and < 1 s, respectively. For some pulses there is an almost one-to-one correspondence between HXR and 48 GHz sub-second pulses. Our findings are consistent with the TOF flare model with collisional trapping playing little role. After Brown, Conway, and Aschwanden (1998) this implies that acceleration time scales to MeV energies are much shorter than the time resolution of the HXR data. Alternative explanations of our results involve, for example, time- and energy-dependent forms of electron acceleration spectrum variations (Brown, Conway, and Aschwanden, 1998) or the existence of compact synchrotron sources with inverse Compton losses (Kaufmann *et al.*, 1986). Further comparisons of HXR and cm–mm radio observations made with high sensitivity, millisecond time resolution and possibly spatial resolution are needed to investigate these different possibilities. This will be soon at hand with the new observations that will be provided, in particular, by the Solar Sub-Millimeter Wave Telescope, the upgrade of the Itapetinga 48 GHz multiple beam focal array, and the High Energy Solar Spectroscopic Imager (HESSI) that will be in operation during the next solar maximum.

Acknowledgements

We acknowledge an anonymous referee for his useful comments. CRAAE is a joint center between Brazilian institutions Mackenzie, INPE, USP and Unicamp. This research received support from the program for exchange of scientists of Brazilian agency CNP_q and French agency CNRS, and partial support from Brazilian agencies FAPESP (Procs. 93/3321-7, 95/9250-6, 96/06956-1, 97/09691-1) and CNP_q (Proc. 150087/96-9), and Switzerland NSF.

References

Aschwanden, M. J.: 1998, *Astrophys. J.* **502**, 455.
Aschwanden, M. J., Schwartz, R. A., and Alt, D. M.: 1995, *Astrophys. J.* **447**, 923.
Aschwanden, M. J., Schwartz, R. A., and Dennis, B. R.: 1998, *Astrophys. J.* **502**, 468.
Brown, J. C., Conway, A. J., and Aschwanden, M. J.: 1998, *Astrophys. J.* **509**, 911.

Correia, E., Costa, J. E. R., Kaufmann, P., Magun, A., and Herrmann, R.: 1995, *Solar Phys.* **159**, 143.
Costa, J. E. R., Brown, J. C., Correia, E., and Kaufmann, P.: 1990, *Astron. Astrophys. Suppl.* **73**, 191.
Costa, J. E. R., Correia, E., Kaufmann, P., Magun, A., and Herrmann, R.: 1995, *Solar Phys.* **159**, 157.
Desai, U. D., Kouveliotou, Ch., Barat, C., Hurley, K., Niel, M., Talon, R., Vedrenne, G., Estulin, I. V., and Dolidze, V. Ch.: 1987, *Astrophys. J.* **319**, 567.
Duijveman, A., Hoyng, P., and Machado, M. E.: 1982, *Solar Phys.* **81**, 137.
Emslie, A. G.: 1983, *Astrophys. J.* **371**, 267.
Forrest, D. J. and Chupp, E. L.: 1983, *Nature* **305**, 291.
Giménez de Castro, C. G., Raulin, J.-P., Makhmutov, V. S., Kaufmann, P., and Costa, J. E.R.: 1999, *Astron. Astrophys. Suppl.* **140**, 373.
Georges, C. B., Schaal, R. E., Costa, J. E. R., Kaufmann, P., and Magun, A.: 1989, *Proc. 2nd Int. Microwave Symp.*, Rio de Janeiro, p. 447.
Herrmann, R., Magun, A., Costa, J. E. R., Correia, E., and Kaufmann, P.: 1992, *Solar Phys.* **142**, 157.
Hurley, K., Niel, M., Talon, R., Estulin, I. V., and Dolidze, V. C.: 1983, *Astrophys. J.* **265**, 1076.
Kane, S. R., Fenimore, E. E., Klebesadel, R. W., and Laros, J. G.: 1982, *Astrophys. J.* **254**, L53.
Kaufmann, P.: 1985, *Solar Phys.* **102**, 97.
Kaufmann, P.: 1996, in R. Ramaty, N. Mandzhavidze, and X.-M. Hua (eds.), *High Energy Solar Physics*, AIP Conference Proc., p. 374.
Kaufmann, P., Strauss, F. M., Opher, R., and Laporte, C.: 1980, *Astron. Astrophys.* **87**, 58.
Kaufmann, P., Strauss, F. M., Schaal, R. E., and Laporte, C.: 1982, *Solar Phys.* **78**, 389.
Kaufmann, P., Correia, E., Costa, J. E. R., Zodi Vaz, A. M., and Dennis, B. R.: 1985, *Nature* **313**, 380.
Kaufmann, P., Correia, E., Costa, J. E. R., and Zodi Vaz, A. M.: 1986, *Astron. Astrophys.* **157**, 11.
Kiplinger, A. L., Dennis, B. R., Emslie, A. G., Frost, K. J., and Orwig, L. E.: 1983, **265**, L99.
Klein, K.-L. and Trottet, G.: 1984: *Astron. Astrophys.* **141**, 67.
Kundu, M. R., White, S. M., Gopalswamy, N., and Lim, J.: 1994, *Astrophys. J. Suppl.* **90**, 599.
Kurt, V., Akimov, V. V., and Leikov, N. G.: 1996, in R. Ramaty, N. Mandzhavidze, and X. M. Hua (eds.), *High Energy Solar Physics*, AIP Conf. Proc. 374, p. 237.
MacKinnon, A. L., Brown, J. C., Trottet, G., and Vilmer, N.: 1983, *Astron. Astrophys.* **119**, 297.
Machado, M. E., Ong, K. K., Emslie, A. G., Fishman, G. J., Meegan, C., Wilson, R., and Paciesas, W. S.: 1993, *Adv. Space Res.* **13** (9), 175.
Masuda, S., Kosugi, T., Hara, H., Tsuneta, S., and Ogawara, Y.: 1994, *Nature* **371**, 495.
McClements, K. G. and Brown, J. C.: 1986, *Astron. Astrophys.* **165**, 235.
Miller, J. A., Cargill, P. J., Emslie, G. A., Holman, G. D., Dennis, B. R., LaRosa, T. N., Winglee, R. M., Benka, S. G., and Tsuneta, S.: 1997, *J. Geophys. Res.* **102** (A7), 14,631.
Pelaez, F., Mandrou, P., Niel, M., Mena, B., Vilmer, N., and Trottet, G.: 1992, *Solar Phys.* **140**, 121.
Pendleton, G., Paciesas, W. S., Mallozzi, R. S. *et al.*: 1995, Nucl. Instr. Method Phys. Res. A **364**, 567.
Ramaty, R., Schwartz, R., Enome, S., and Nakajima, H.: 1994, *Astrophys. J.* **436**, 941.
Raulin, J.-P., Kaufmann, P., Olivieri, R., Correia, E., Makhmutov, V. S., and Magun, A.: 1998, *Astrophys. J.* **498**, L173.
Raulin, J.-P., White, S. M., Kundu, M. R., Silva, A. V. R., and Shibasaki, K.: 1999, *Astrophys. J.* **522**, 547.
Raulin, J.-P., Vilmer, N., Trottet, G., Nitta, N., Silva, A. V. R., Kaufmann, P., Correia, E., and Magun, A.: 2000, *Astron. Astrophys.*, in press.
Sakao, T.: 1994, PhD. Thesis, University of Tokyo, Tokyo, Japan.
Sakao, T., Kosugi, T., Masuda, S., Inda, M., Makishima, K., Canfield, R. C., Hudson, H. S., Metcalf, T. R., Wülser, J.-P., Acton, L. W., and Ogawara, Y.: 1992, *Publ. Astron. Soc. Japan* **44**, L83.
Takakura, T., Kaufmann, P., Costa, J. E. R., Degaonkar, S. S., Ohki, K., and Nitta, N.: 1983, *Nature* **302**, 5906.

Talon, R., Barat, C., Dezalay, J.-P., Vilmer, N., Trottet, G., Sunyaev, R., Terekhov, O., and Kuznetsov, A.: 1993, *Adv. Space Res.* **13** (9), 171.
Trottet, G. and Vilmer, N.: 1984, *Adv. Space Res.* **4** (2–3), 153.
Trottet, G., Vilmer, N., Barat, C., Benz, A. O., Magun, A., Kuznetsov, A., Sunyaev, R., and Tereekhov, O.: 1998, *Astron. Astrophys.* **334**, 109.
Vestrand, W. T.: 1988, *Solar Phys.* **118**, 95.
Vilmer, N.: 1987, *Solar Phys.* **111**, 207.
Vilmer, N. and Trottet, G.: 1997, in G. Trottet (ed.), *Coronal Physics from Radio and Space Observations*, Lect. Notes Phys. No. 483, p. 28.
Vilmer, N., Trottet, G., and Mackinnon, A. L.: 1986, *Astron. Astrophys.* **156**, 64.
Vilmer, N., Trottet, G., Barat, C., Dezalay, J. P., Talon, R., Sunyaev, R., Terekhov, O., and Kuznetsov, A.: 1994, *Space Sci. Rev.* **68**, 233.
Vilmer, N., Trottet, G., Verhagen, H., Barat, C., Talon, R., Dezalay, J. P., Sunyaev, R., Terekhov, O., and Kuznetsov, A.: 1996, *AIP Conf. Proc.* **374**, 311.
Vilmer, N., Trottet, G., Barat, C., Benz, A. O., Magun, A., Kuznetsov, A., Sunyaev, R., and Tereekhov, O.: 1999, *Astron. Astrophys.* **342**, 575.
White, S. M., Kundu, M. R., Bastian, T. S., Gary, D. E., Hurford, G. J., Kucera, T., and Bieging, J. H.: 1992, *Astrophys. J.* **384**, 656.
Zodi Vaz, A. M., Kaufmann, P., Correia, E., Costa, J. E. R., Cliver, E. W., Takakura, T., and Tapping, K. F.: 1985, *Rapid Fluctuations in Solar Flares*, NASA Conf. Publ., 2449, p. 171.